

# Dynamic Poly(3,4-ethylenedioxythiophene)s Integrate Low Impedance with Redox-Switchable Biofunction

Hsing-An Lin, Bo Zhu,\* Yu-Wei Wu, Jun Sekine, Aiko Nakao, Shyh-Chyang Luo,\* Yoshiro Yamashita,\* and Hsiao-Hua Yu\*

To generate the electrical communication, biocompatibility, and controlled cell attachment properties required for advanced bioelectronic technologies, a dynamic poly(3,4-ethylenedioxythiophene) (PEDOT) film is developed based on a biomimetic approach. The dynamic PEDOT integrates low impedance, nonspecific-binding resistance, and redox-responsive characteristics while coupling with cells stably and specifically. The combination of these features ensures stable and efficient electrical communication with cells and promises potentially reduced disruption of complexes in physiological environments due to the material's strong resistance to nonspecific interactions; more significantly, the integration of these features in one material enables the spatiotemporal attachment and detachment of cells on demand without damage to cell viability and neurites after 5 d of electrical stimulation and culturing. The dynamic and biomimetic PEDOT material can be an ideal electronic interface with optimized electrochemical and biological characteristics toward biocompatible and controllable electrocoupling with cells at low impedance.

signals.<sup>[5,6]</sup> Furthermore, the use of bioelectronics as tissue scaffolds can electrically initiate the regeneration of limbs and spinal cords<sup>[7,8]</sup> and accelerate wound healing.<sup>[9]</sup> With the progress of bioelectronics toward cell–device communication at high signal-to-noise ratios and spatial resolutions and with flexible architectures and small sizes, the next generation of bioelectronic materials requires low impedance, sufficient biofunction, and appropriate flexibility to meet the required electrical communication,<sup>[10,11]</sup> biocompatibility,<sup>[12,13]</sup> and mechanical strength<sup>[14,15]</sup> demands for interfacing with cells and tissues. The traditional materials for bioelectronics, such as metals and silicon, however, do not fully satisfy the aforementioned requirements. In addition, when these devices evolve toward smaller sizes, sustaining efficient electrical communication

using metals and silicon as electrode materials would be challenging because the reduction in the sizes of recording sites normally increases impedance.<sup>[16]</sup>

Poly(3,4-ethylenedioxythiophene) (PEDOT) has a 1 kHz interfacial impedance, which is significantly lower than those of platinum<sup>[17]</sup> and iridium oxide,<sup>[11]</sup> and a much smaller

## 1. Introduction

Bioelectronics, integrating (bio)materials and circuits, provide new tools for life science studies and the development of new therapy methods. For example, bioelectronics can develop as neural prostheses to substitute damaged motor or sensory modalities<sup>[1–4]</sup> or act as biosensors to monitor biological


Dr. H.-A. Lin, Prof. B. Zhu, Dr. Y.-W. Wu, J. Sekine, Prof. S.-C. Luo,  
Dr. H.-H. Yu

Responsive Organic Materials Laboratory  
RIKEN

Wako, Saitama 351-0198, Japan  
E-mail: bozhu@shu.edu.cn; shyhchyang@ntu.edu.tw;  
bruceyu@gate.sinica.edu.tw

Dr. H.-A. Lin, Prof. Y. Yamashita  
Department of Electronic Chemistry  
Interdisciplinary Graduate School of Science and Engineering  
Tokyo Institute of Technology  
Yokohama, Kanagawa 226-8502, Japan  
E-mail: yoshiro@echem.titech.ac.jp

Prof. B. Zhu  
State Key Laboratory for Modification of Chemical Fibres  
and Polymer Materials  
College of Materials Science and Engineering  
Donghua University  
2999 Renmin North Road, Songjiang, Shanghai 201600, China

 The ORCID identification number(s) for the author(s) of this article can be found under <https://doi.org/10.1002/adfm.201703890>.

Prof. B. Zhu  
College of Materials Science and Engineering  
Shanghai University  
99 Shangda Road, Baoshan, Shanghai 200444, China

Dr. Y.-W. Wu  
Brain Science Institute  
RIKEN  
Wako, Saitama 351-0198, Japan

Dr. A. Nakao  
Bio-Engineering Laboratory  
RIKEN  
Wako, Saitama 351-0198, Japan

Prof. S.-C. Luo  
Department of Materials Science and Engineering  
National Taiwan University  
No. 1, Sec. 4, Roosevelt Road, Taipei 10617, Taiwan

Dr. H.-H. Yu  
Institute of Chemistry  
Academia Sinica  
128 Academic Road, Sec. 2, Nankang, Taipei 11529, Taiwan

DOI: 10.1002/adfm.201703890

stiffness than metallic materials, which reduces mechanical mismatch with cells.<sup>[18]</sup> When assembled into nanostructures, its impedance can even decrease by two orders of magnitude.<sup>[19]</sup> Furthermore, PEDOT electrodes have excellent electrochemical stability in aqueous solution,<sup>[20–23]</sup> a high charge injection limit,<sup>[24,25]</sup> and low potential excursion,<sup>[11,26]</sup> which all ensure that PEDOT electrodes can stably deliver charge. PEDOT electrodes have already demonstrated excellent electrical stimulation and recording performances in many bioelectronic devices, both *in vitro*<sup>[27–30]</sup> and *in vivo*.<sup>[31–35]</sup>

However, PEDOT also nonspecifically binds proteins and cells or induces gliosis when operating in a physiological environment.<sup>[31,36]</sup> As a result, PEDOT suffers from a large increase in impedance and a much-abated communication performance.<sup>[37]</sup> Grafting biomolecules onto PEDOT is considered an efficient strategy to improve its biocompatibility.<sup>[38]</sup> Although a few studies showed that impedance of PEDOTs remains unchanged after the functionalization,<sup>[39,40]</sup> sustaining the low impedance of PEDOTs generally remains challenging, as the incorporation of functional molecules normally reduces PEDOT conductivity by distorting its backbone or introducing insulating side-chains. To generate biocompatible PEDOT materials with low impedance via an alternative approach, we developed a cell membrane-mimicking 3,4-ethylenedioxythiophene (EDOT)-based polymer that recognizes cells but without nonspecific binding.<sup>[41]</sup> This biomimetic PEDOT material uniquely combines a low impedance with a specific biofunction and promises stable communication between devices and a specific physiological target.

Endowing PEDOT with a dynamic control of biofunctions can realize the spatiotemporal control of cell interactions and electrical communication, which are highly desired for many bioelectronics and biomedical applications, such as neural probes and tissue regeneration/transplantation.<sup>[42,43]</sup> Applying external stimuli, including electrical,<sup>[44,45]</sup> thermal,<sup>[46]</sup> light,<sup>[47]</sup> and pH stimuli,<sup>[48]</sup> to cell-culture platforms have demonstrated that these strategies can manipulate the surface functions of the platforms to control cell attachment/detachment. For example, a sulfonic acid-functionalized EDOT polymer recently demonstrated spatiotemporal control of cell detachment by electrically degrading the cross-linkage in PEDOT.<sup>[49,50]</sup> The integrity of the cell membrane was maintained compared with that of traditional trypsinization. Both studies have demonstrated the superior performance of an electrotuned cell attachment technique. To achieve spatiotemporal electrotuning of cell interactions by an alternative strategy, we equipped a PEDOT material with a bioactive ligand that contains an electrical switch and applied a potential as an external stimulus to rationally turn the biofunction of PEDOT on and off to realize selective cell interactions with electrotunable cell attachment.

With concern for the aforementioned issues of electrical communication, biocompatibility, and electroswitchable cell attachment, we aim to fabricate an organic electronic biomaterial that also has low impedance, protein resistance, and redox-responsive cell-coupling. We have demonstrated that our cell membrane-mimicking PEDOT can function as a smart electrode to selectively couple with nerve cells and allows efficient electrical communication over long periods of time to promote cell differentiation.<sup>[41]</sup> Taking advantage of this biomimetic

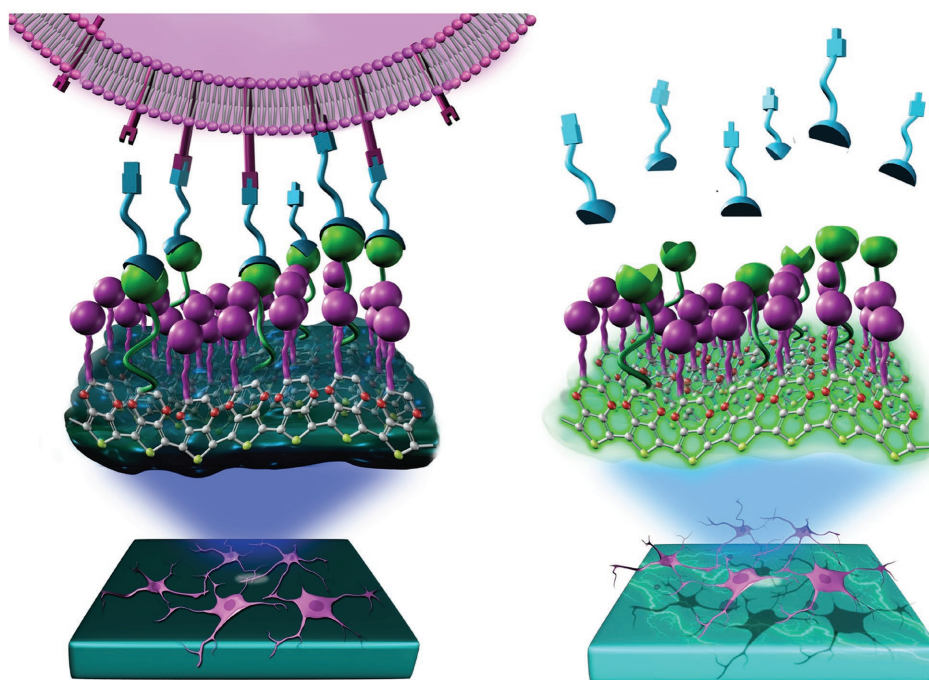
PEDOT and a cue from the structure of phospholipids, we design and synthesize a dynamic PEDOT material that consists of a phosphorylcholine-grafted EDOT to prevent nonspecific binding to cells and proteins and a hydroquinone-grafted EDOT as a redox switch for controlled conjugation with peptide ligands to mimic specific integrin-extracellular matrix (ECM) interactions. (Schemes 1 and 2). The dynamic PEDOT material possesses low impedance, a resistance toward nonspecific interactions, and, more important, a redox-responsive function that controls physical and electrical coupling with targeted cells through an applied programmed sequence of potentials. Utilizing this dynamic PEDOT material, we show that efficient and stable electrical communication can be achieved between an electrode and cells. A short and very low reduction potential can quickly release electrically differentiated neuron model cells with high viability and morphological integrity after 5 d of stimulation and culture. We envision this intriguing PEDOT material a promising candidate for electronic devices to specifically electrocouple to cells at low impedance and to provide spatiotemporal control over both the attachment and detachment of targeted cells.

## 2. Results and Discussion

### 2.1. Design and Synthesis of the Redox-Responsive PEDOT

Considering chemical stability and fabrication simplicity, our strategy to meet the electroswitchable constraint focuses on introducing redox-responsive conjugation linkages to PEDOT. In photosystem II of green plants, the quinone/quinol redox couple transports electrons between membrane proteins by a redox reaction, thereby coupling electron transfer to transmembrane proton-gradient formation.<sup>[51]</sup> The reversible redox reaction of quinones and its intrinsic role in electron and proton transfer have been clarified.<sup>[52]</sup> Quinone molecules and their derivatives were recently used as doping ions to dramatically enhance the charge storage of electrodes<sup>[53]</sup> and also self-assembled as a monolayer to achieve controllable conjugation with molecules and subsequent interactions with cells.<sup>[54]</sup> Inspired by the redox relays of photosystem II and previous achievements, we used the hydroquinone (HQ)/benzoquinone (BQ) redox couple as a redox switch to control the conjugation of functional molecules with PEDOT electrodes. Using a bottom-up approach, we synthesized EDOT building blocks bearing HQ groups hydroquinone-functionalized EDOT (EDOT-HQ) and electropolymerized them into poly(EDOT-HQ) films by simply applying the optimized oxidation potential. In the following investigation, we utilize oxime ligation to immobilize amino-terminated molecules onto the polymer surface, as the oxime linkage is stable under physiological conditions but can be cleaved at a certain reduction potential.<sup>[55]</sup>

Our synthetic approach for creating EDOT-HQ is presented **Scheme 3**. A care should be taken to prevent the oxidation of HQ molecules. We used <sup>1</sup>H and <sup>13</sup>C NMR and mass spectrometry to confirm the structure of the functionalized EDOT monomer. The signal of the OH groups of the HQ unit was clearly evident in the <sup>1</sup>H NMR spectrum, while the measured mass of the monomer was consistent with its expected exact mass.



**Scheme 1.** Schematic presentation of electrical communication and redox-triggered interactions between neurons and a dynamic PEDOT material functionalized with hydroquinone electroswitches and phosphorylcholine zwitterions. When functionalized by RGD peptides on the surface through oximation under electro-oxidation conditions, the dynamic PEDOT film provides a stable support and an efficient electrical interface for neurons (left); it gently detaches cells as a response to the electroreductive cleaving of bonds between the peptides and the surface (right).

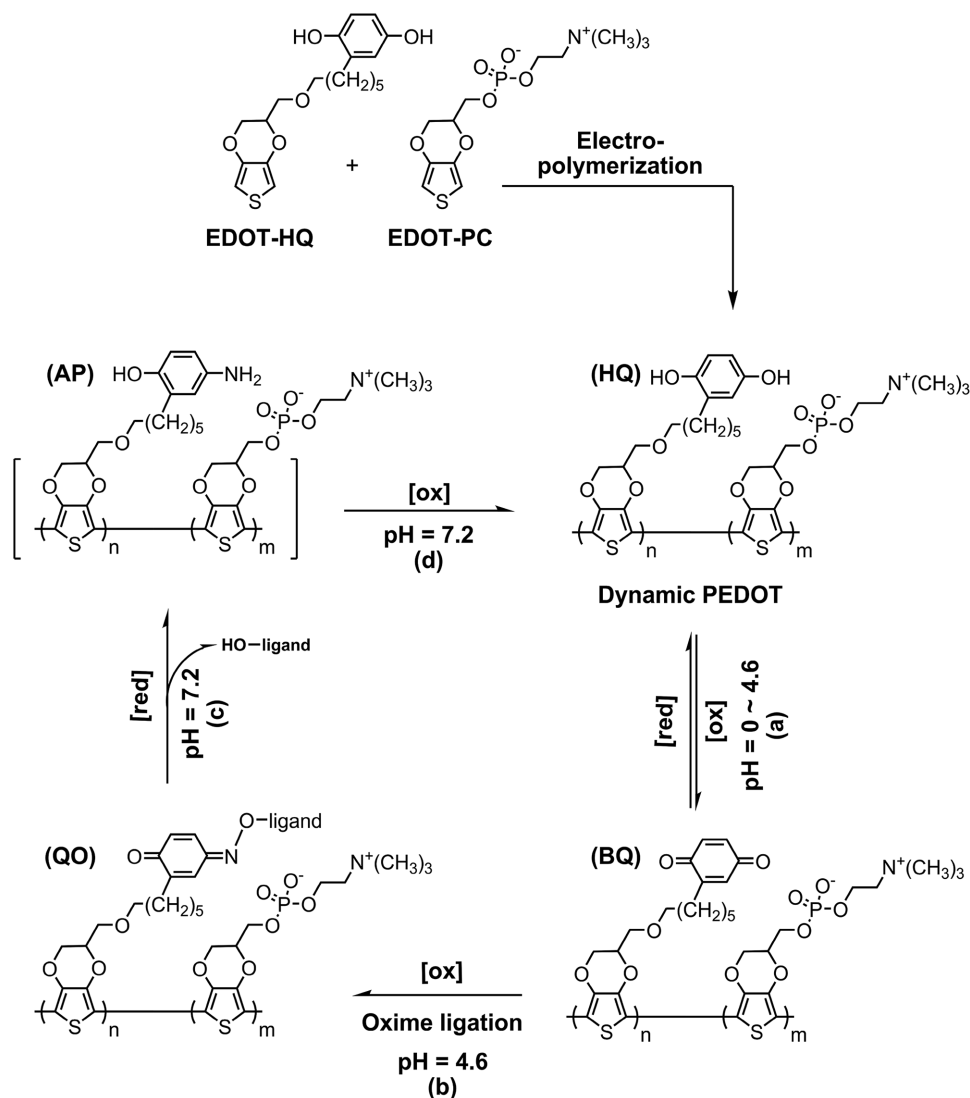
To prepare poly(EDOT-HQ) films on Au-dish electrodes, we applied a potential that cycled from  $-0.3$  to  $+1.1$  V to an acetonitrile solution containing  $0.01$  M EDOT-HQ and  $0.1$  M  $\text{LiClO}_4$ . Unfunctionalized PEDOT films on Au-dish electrodes were prepared in the same manner to function as a control. Typical voltammograms obtained upon electropolymerization of EDOT-HQ are shown in **Figure 1a**. The initial anodic sweep featured an anodic peak for the oxidation of EDOT-HQ at  $0.84$  V (vs  $\text{Ag}/\text{Ag}^+$ ). The reverse scan yielded cathodic peaks at  $0.37$  and  $0.10$  V, which we assigned to the reduction of BQ.<sup>[52]</sup> In the second and subsequent scans of EDOT-HQ electropolymerization, a new anodic shoulder appeared near  $0.62$  V. In contrast, the electropolymerization of EDOT-OH does not give similar anodic and cathodic peaks (**Figure 1b**).

## 2.2. HQ/BQ Redox Switching in PEDOT-HQ

The HQ unit has pH-dependent electrochemical behavior, and its redox properties highly depend on the type and pH value of solutions.<sup>[52]</sup> To ensure redox switching of the HQ pendant unit, we investigated cyclic voltammetry of the poly(EDOT-HQ) film in  $1$  M  $\text{HClO}_4$  (pH 0). The electrochemical stimuli-induced switching behavior of a poly(EDOT-HQ) film is summarized in **Figure 2**. The HQ unit underwent the redox cycle presented in **Figure 2a**. A sharp anodic peak appeared at  $0.59$  V (vs  $\text{Ag}/\text{AgCl}$ ) during the anodic sweep cycle, indicating that the HQ unit had been oxidized to form BQ,<sup>[56]</sup> as shown in **Figure 2b**. In the cathodic sweep, a much broader peak appeared from  $0.4$  to  $0.18$  V due to the reduction of BQ to HQ. To confirm that these

peaks did indeed represent HQ/BQ switching, we also measured a cyclic voltammogram of a poly(EDOT-OH) film under the same conditions as those used to measure the poly(EDOT-HQ) film. We observed only broad anodic and cathodic peaks without the signature peaks for the HQ/BQ transitions. Thus, the anodic and cathodic peaks in the cyclic voltammogram of poly(EDOT-HQ) correspond to redox transformations of the HQ units on the PEDOT backbone.

To further understand the HQ/BQ switching behavior of the polymer film in aqueous solutions, we electrodeposited a poly(EDOT-HQ) film onto indium tin oxide (ITO)-coated quartz and examined its spectroelectrochemical performance. **Figure 2c** displays the optical properties of the poly(EDOT-HQ) film subjected to constantly applied voltages of  $-0.3$  and  $+0.7$  V in  $1$  M  $\text{HClO}_4$ . When we applied a potential of  $+0.7$  V to the poly(EDOT-HQ) film, we observed absorbances at  $255$ ,  $290$ , and  $355$  nm. An absorbance peak at  $255$  nm should correspond to the absorbance of the BQ units.<sup>[57]</sup> When we changed the applied potential from  $+0.7$  to  $-0.3$  V, only one absorbance peak—at  $288$  nm—appeared in the spectrum; we assigned it to HQ units. To examine the reversibility of the HQ/BQ switch, we monitored the absorbance at  $255$  nm (from BQ) and  $288$  nm (from HQ) over ten cycles of switching in the potential range from  $-0.3$  to  $+0.7$  V, as shown in **Figure 2d**. An initial potential of  $-0.3$  V was applied to the polymer film for 2 min to ensure that it began the cycling process in the reduced state (HQ moieties). When we increased the potential from  $-0.3$  to  $+0.7$  V, the absorbance at  $255$  nm increased and that at  $288$  nm decreased, consistent with the oxidation of the HQ units to form BQ units during the oxidation scan. In contrast,



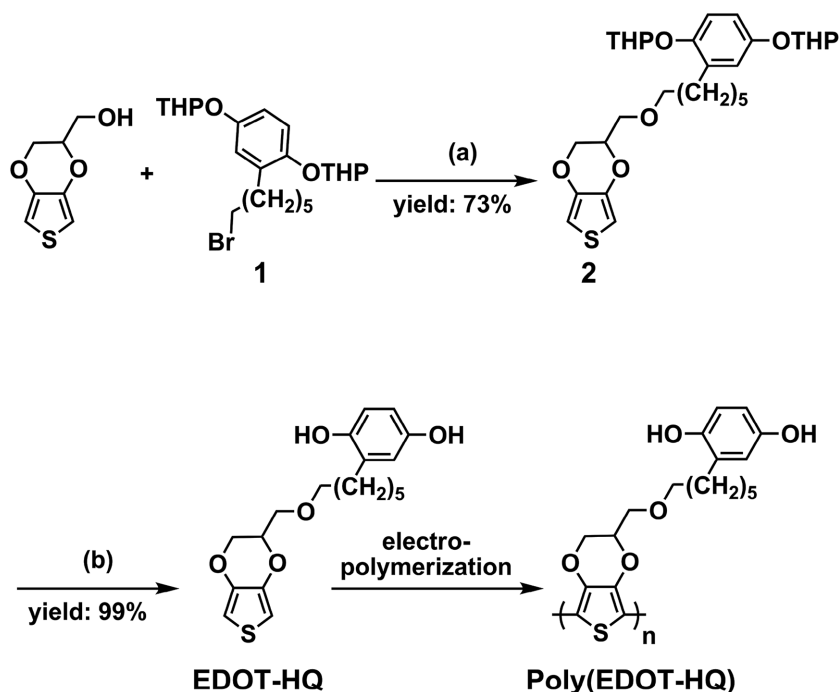
**Scheme 2.** Constructing dynamic PEDOT and its electroswitchable biofunctions by sequential potential application and bioconjugation chemistry. a) Redox switching between HQ/BQ; b) turning on biofunction of dynamic PEDOT through immobilization of bioactive ligands under electrooxidation; c) turning off biofunction of dynamic PEDOT through cleavage of quinone oxime (QO) linkages between the ligands and the surfaces; d) regeneration of HQ from aminophenol (AP) through electrooxidation.

the BQ units were reduced to form HQ units during the reduction scans, as confirmed by the increased absorbance at 288 nm and decreased absorbance at 255 nm. The changes in absorbance intensities at 255 and 288 nm were very stable, and the switching was very regular during the ten cycles of applied voltages. The poly(EDOT-HQ) film thus displayed both electrically controllable switching of its HQ units and reversible HQ/BQ switching in an aqueous solution.

### 2.3. Spatiotemporal Capture and Release of Fluorophores on PEDOT-HQ Microarrays

Oxime ligation could be an efficient strategy for switching functions on and off, thereby controlling the conjugation of molecules and their release from poly(EDOT-HQ) films. The HQ unit underwent the redox cycle and the formation/cleavage of

oxime linkages on poly(EDOT-HQ) films, as shown in **Figure 3a**. Poly(EDOT-HQ) was first oxidized to form poly(EDOT-BQ) in pH 4.6 acetate buffer. The aminoxy-containing ligands (in the acetate buffer) were immobilized on poly(EDOT-HQ) films through oxime conjugation. The formed quinone oxime (QO) linkage could be electrochemically reduced to form an aminophenol (AP) unit and release a hydroxyl-terminated molecule (ligand-OH) under physiological conditions (pH 7.2 phosphate-buffered saline (PBS)), and an HQ unit could then be regenerated from the AP by subsequently applying an oxidative potential.<sup>[55]</sup> Here, we cleaved the oxime linkages in pH 7.2 PBS buffer, and not in an acidic buffer, because when poly(EDOT-HQ) films or HQ-containing polymer films operate in biological environments for bioengineering applications, the polymer films must cleave the oxime linkage to release the immobilized ligands. To demonstrate the programmable immobilization of molecules on poly(EDOT-HQ) films and their subsequent



**Scheme 3.** Synthesis of EDOT-HQ monomer and its polymer poly(EDOT-HQ). Reaction conditions: **1** (1.0 equiv), NaH (5.0 equiv), 18-crown-6 ether (0.1 equiv), THF, 0 °C to r.t., overnight; b) Acetic acid/THF/water (3/1/1), r.t., 4 h. THP = tetrahydropyran.

release therefrom, we employed interdigitated microelectrodes to selectively address the electrodes electrochemically, as shown in Figure 2b. We first used the aforementioned electropolymerization conditions to deposit poly(EDOT-HQ) polymers onto both microelectrodes to obtain poly(EDOT-HQ) microelectrodes that were interdigitated with each other (with two sets of gold working electrodes: WE1 and WE2). After applying an oxidative potential of 0.7 V on the electrode, we could selectively immobilize aminoxy-functionalized Alexa-488 dyes onto it. To ensure high spatial resolution and contrast in the fluorescent images, we used two-photon microscopy because it uses a laser that excites fluorophores via two near-simultaneous long-wavelength photons and that excitation is only achieved near the focal plane where the laser light is most concentrated. Through selective application of oxidation potentials to WE1

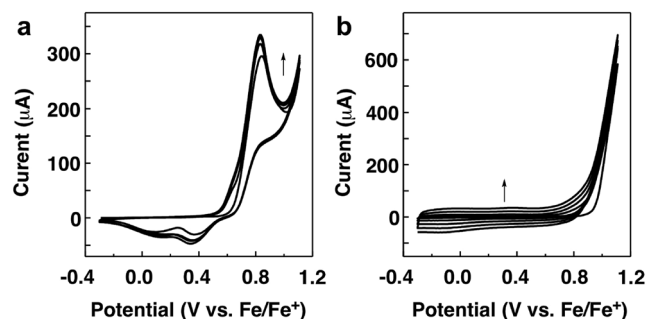


**Figure 1.** Electropolymerization of a) EDOT-HQ ( $10 \times 10^{-3}$  M) and b) EDOT ( $10 \times 10^{-3}$  M) in MeCN containing  $100 \times 10^{-3}$  M LiClO<sub>4</sub>; five scans at a scan rate of 100 mV s<sup>-1</sup>.

and/or WE2 to oxidize the HQ units, we achieved successful immobilization of Alexa dyes on a single set or both sets of working electrodes. Most importantly, we could selectively release the immobilized Alexa dyes by applying a reductive potential of -0.05 V on WE2 (in PBS buffer for 15 min). Figure 3b shows the spatiotemporal capture and release of functional molecules by poly(EDOT-HQ) microelectrodes that are responding to fine-tuned electrochemical signals.

In addition, the cleavage of oxime linkages and the regeneration of HQ from AP were investigated by cyclic voltammetry. A poly(EDOT-QO) film was prepared on an Au-dish electrode, and a reductive potential (-0.05 V) and a subsequent oxidative potential (0.7 V), were then applied to the film in pH 7.2 PBS buffer. The cyclic voltammograms of a pristine poly(EDOT-QO) film and a regenerated poly(EDOT-HQ) film are shown in Figure S1 in the Supporting Information. The pristine poly(EDOT-QO) film exhibited a sharp anodic peak at 0.63 V (vs Ag/AgCl) and a cathodic peak at 0.49 V, which corresponds to formation of oxime linkages on the polymer surface.<sup>[58]</sup> After sequential reductive and oxidative potentials

were applied to poly(EDOT-QO) films, the original anodic peak shifted from 0.63 to 0.6 V, and the cathodic peak at 0.49 V disappeared, which indicate that the cleavage of oxime linkages and the regeneration of HQ were successfully performed on the poly(EDOT-QO) films. Our results suggest that poly(EDOT-HQ) has great potential to switch functions on and off in bioelectronic devices, thereby controlling electrode-cell interactions.

#### 2.4. Dynamic PEDOT Integrating Resistance to Nonspecific Interactions and Low Impedance

To fully functionalize the switch and control electrode-cell interactions in a physiological environment, we must stop PEDOT from disrupting proteins and cells by nonspecifically binding them. Not only that, but nonspecific interactions would lead to binding of nontargeted proteins and cells or gliosis and increase the impedance, abating the communication performance of electrodes. To eliminate nonspecific binding, we integrated cell-resistant phosphorylcholine-functionalized EDOT (EDOT-PC) with electroresponsive EDOT-HQ to synthesize a biomimetic PEDOT copolymer. The resistance of phosphorylcholine groups to nonspecific adhesion to both proteins and cells most likely arises from the highly hydrophilic yet net-neutral properties of the zwitterionic groups. Phosphorylcholine side-chains on surfaces can efficiently prevent microphages from recognizing artificial implants as foreign bodies, leading to diminution/eradication of the inflammatory response.<sup>[59]</sup> Due to the absence of nonspecific protein/cell-binding, cell-electrode interactions could be solely based on specific interactions, and

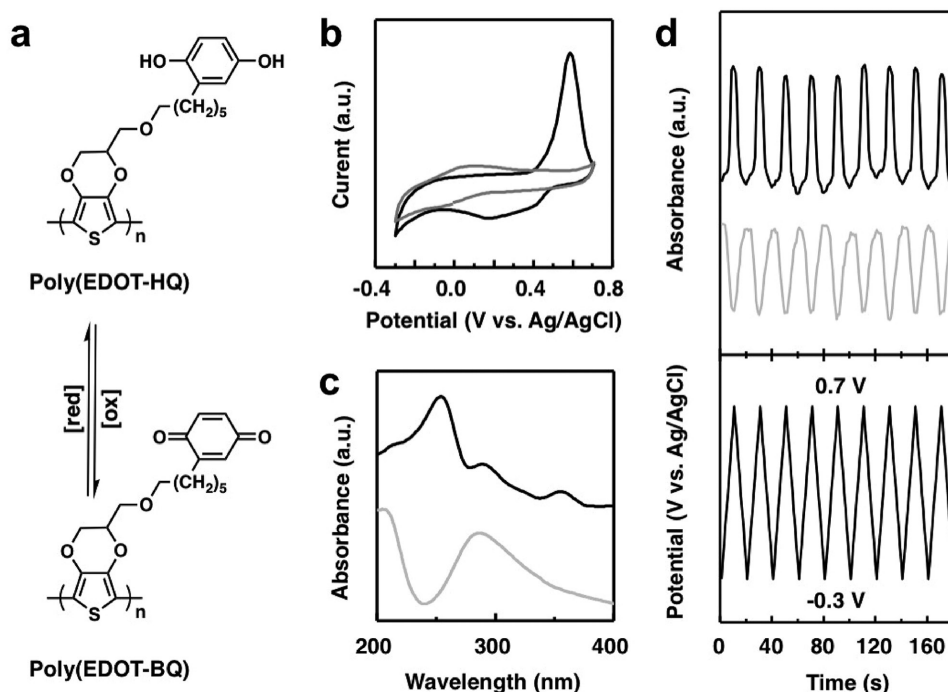


**Figure 2.** a) Schematic illustration of poly(EDOT-HQ)/poly(EDOT-BQ) switching; b) cyclic voltammograms of a poly(EDOT-HQ) film (black line) and a PEDOT film (gray line) on Au electrodes in a 1 M HClO<sub>4</sub> aqueous solution at a scan rate of 100 mV s<sup>-1</sup>; c) UV-vis absorption spectrum of a poly(EDOT-HQ) film on ITO-coated quartz under applied potentials of -0.3 V versus Ag/AgCl (gray line) and +0.7 V versus Ag/AgCl (black line), representing the absorption spectra of poly(EDOT-HQ) and poly(EDOT-BQ) films, respectively. d) In situ UV-vis monitoring (top) of the absorbance at 255 nm from the BQ unit (black line) and at 288 nm from the HQ unit (gray line) over ten cycles of switching (bottom) within the potential range of -0.3 to +0.7 V versus Ag/AgCl.

a controlled attachment and release of targeted cells could thus be realized through programming the electrochemical signal to conjugate and cleave an integrin-recognizing peptide sequence.

To ensure copolymerization of the immiscible EDOT-PC and EDOT-HQ monomers, we employed inverse microemulsion electropolymerization (which we had developed),<sup>[41]</sup> resulting in cell-resistant copolymer films of poly(EDOT-HQ-co-EDOT-PC) on conductive substrates. This method allowed EDOT-PC and EDOT-HQ to copolymerize as films within an EDOT-HQ feed composition (molar percentage within the monomer mixture) range from 0% to 30%. To determine the compositions of the copolymer films, high-resolution X-ray photoelectron spectroscopy (XPS) spectra were measured. The XPS spectra of EDOT-HQ and EDOT-PC both featured signals from the S 2p electrons, but only that of EDOT-PC featured a signal from the N 1s electrons. Therefore, the ratio of the signals from the S 2p and N 1s electrons of each sample, considering their differences in relative sensitivity factor, allowed us to determine the absolute composition of the copolymer films. These results are summarized in Figure S2 in the Supporting Information. Although the measured composition of EDOT-HQ in the films was slightly higher, it exhibited an almost linear relationship with the feed percentage of EDOT-HQ in the monomer mixture, indicating that the composition may be fine-tuned to optimize the properties of the copolymer.

Accordingly, we optimized the composition of our new PEDOT copolymer (i.e., the ratio of EDOT-HQ to EDOT-PC) to obtain high resistance to nonspecific cell binding while maintaining a balanced conjugation density. The surface resistance to

attachment of NIH3T3 cells with respect to the feed ratio of the EDOT-HQ monomer revealed a sigmoidal curve, instead of a linear relationship (Figure 4a). As expected, the poly(EDOT-PC) film is very resistant to NIH3T3 nonspecific binding due to the superhydrophilicity and neutrality of the zwitterionic phosphorylcholine groups. When the feed percentage of EDOT-HQ in the monomer mixture was increased to 15%, the copolymer films retained great resistance to attachment of NIH3T3 cells (Figure 4b). Once the EDOT-HQ content exceeded 15%, however, strong nonspecific interactions between the cells and the copolymer films occurred (Figure 4c). Thus, poly(EDOT-HQ-co-EDOT-PC) samples containing 15% or less EDOT-HQ might be able to control electrode-cell interactions with minimal interference from nonspecific interactions.

Previous efforts to functionalize PEDOT materials by grafting molecules suffered from the loss of low impedance as the incorporation of molecules normally reduced the materials' conductivity by distorting their backbones or introducing insulating side-chains. To compare the impedances of our polymers and PEDOT, the effects of surface roughness and thickness should be considered. We thus used surfactant-assisted electropolymerization to prepare poly(EDOT-PC), poly(EDOT-HQ-co-EDOT-PC) and PEDOT films to ensure that they had similarly smooth surfaces ( $R_{\text{rms}} < 10$  nm). Meanwhile, polymer films of identical thickness were achieved by depositing the same amount of charge within 113 mm<sup>2</sup> of the substrate. As revealed in Figure 4d; Figure S3 in the Supporting Information, the impedance of poly(EDOT-PC) was the same as that of

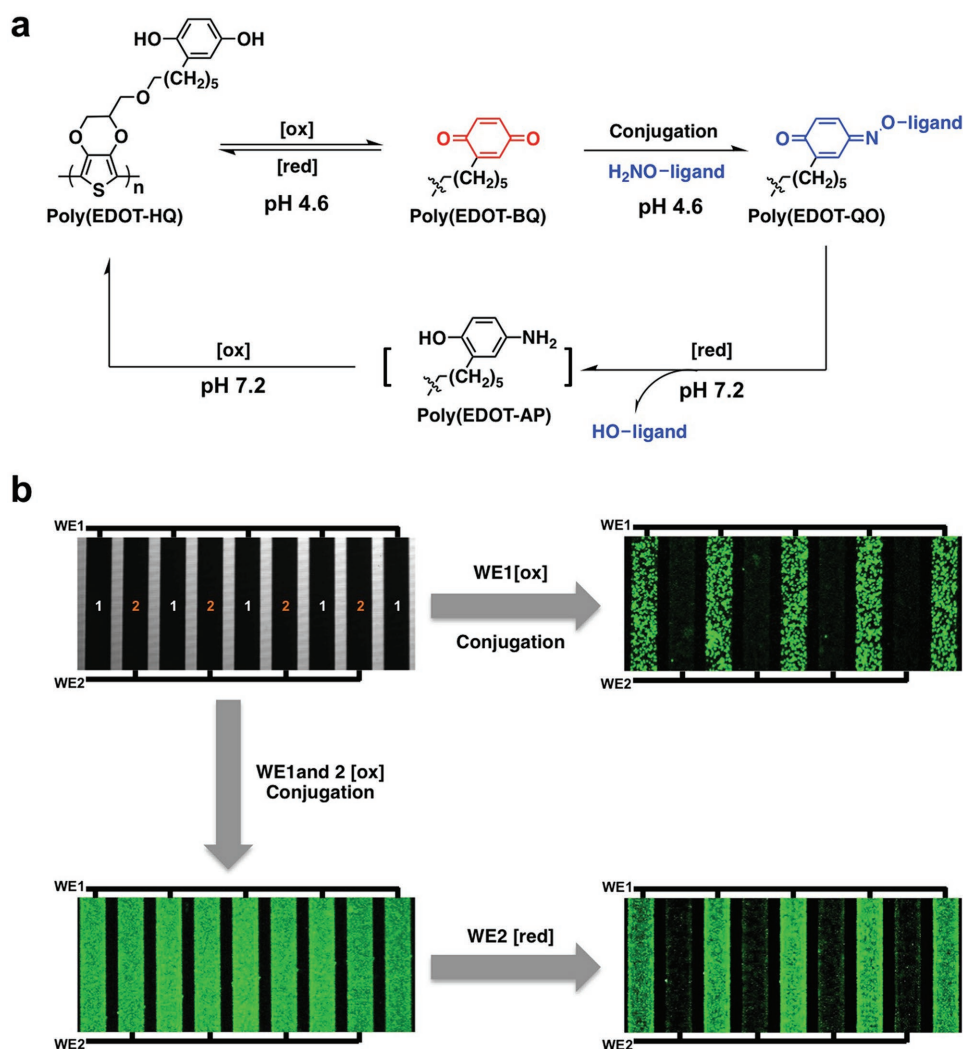


**Figure 3.** a) Schematic illustration of poly(EDOT-HQ)/poly(EDOT-BQ) switching and the formation/cleavage of oxime linkages on poly(EDOT-HQ) films; b) bright-field image of a poly(EDOT-HQ) film coated on two sets of interdigitated Au working microelectrodes (WE1, WE2) (top-left); fluorescence images by two-photon excitation microscopy showing the selective immobilization and release of aminoxy-functionalized Alexa-488 dyes on poly(EDOT-HQ)-coated interdigitated Au microelectrodes. When the oxidative potential was only applied to WE1 to convert poly(EDOT-HQ) to poly(EDOT-BQ), the Alexa dyes were selectively immobilized on WE1 through oxime conjugation (top-right); when the oxidative potential was applied to both WE1 and WE2, Alexa dyes were immobilized on both electrodes (bottom-left). Alexa dyes were selectively released from WE2 by applying a reductive potential to cleave the oxime conjugation (bottom-right).

unfunctionalized PEDOT. That is, the incorporation of phosphorylcholine groups imparts the material with low electrical impedance. The zwitterionic groups contribute to the ionic conductivity, which probably results in this feature.<sup>[60]</sup> The copolymerization of 10% EDOT-HQ very slightly increases the impedance compared to that of pure poly(EDOT-PC). In the low-frequency range, the impedance magnitude is one order lower than that of gold substrate. Our dynamic functional PEDOT materials with low electrical impedance therefore provide good electrical communication between the electrode and cells/tissues.

The peptide GlyArgGlyAspSerPro (GRGDSP) has been widely used to introduce specific cell adhesion on a variety of substrates. We also adopt it here as a model biomolecule to demonstrate the specific function of this dynamic PEDOT

material. To ensure the specific binding of NIH3T3 cells to the originally bioinert poly(EDOT-HQ-co-EDOT-PC) film, we grafted an aminoxy-functionalized RGD peptide (NH<sub>2</sub>O-EG<sub>2</sub>-GRGDSP) to the copolymer film through oxime ligation by electrooxidation at 0.7 V. After the RGD peptides grafted, the bioinert copolymer film strongly interacted with NIH3T3 cells. As expected, the density of the attached NIH3T3 cells increased dramatically when the EDOT-HQ feed composition increased from 0% to 15% in the monomer mixture solution. We compared the cell attachment and subsequent release of all samples and found that the copolymer film that had been deposited from a solution with a 10% feed composition of EDOT-HQ demonstrated an optimized and balanced performance. We thus only show results from this film from this point forward.

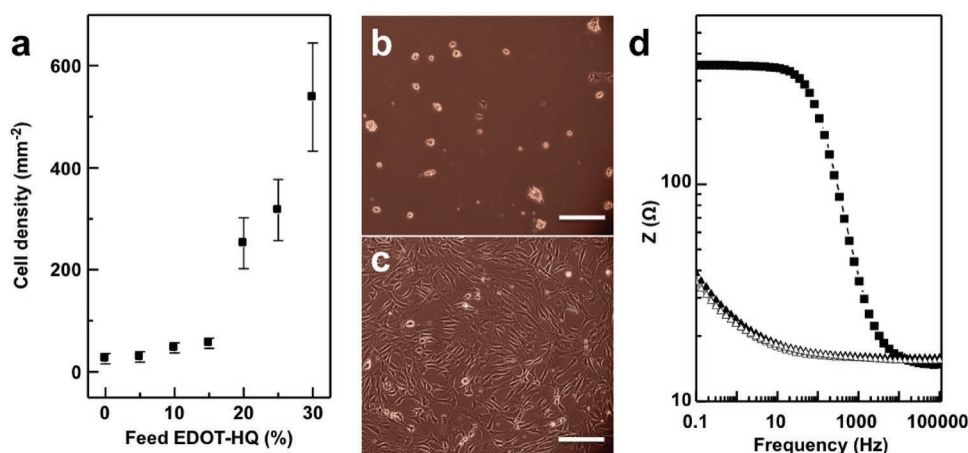


**Figure 4.** a) The cell density of NIH3T3 cells attached to poly(EDOT-HQ-co-EDOT-PC) prepared with different feed compositions of EDOT-HQ. NIH3T3 cells were seeded into serum-containing media at a density of  $1 \times 10^5$  cells mL<sup>-1</sup> and incubated for 12 h; b) bright-field images of NIH3T3 cells seeded onto poly(EDOT-HQ-co-EDOT-PC) films electrocopolymerized at a feed composition of 15% EDOT-HQ and 85% EDOT-PC; c) bright-field images of NIH3T3 cells seeded onto poly(EDOT-HQ-co-EDOT-PC) films electrocopolymerized at a feed composition of 20% EDOT-HQ and 80% EDOT-PC. d) Electrochemical impedance spectra (Bode plots) of a thin Au film (filled square), poly(EDOT-PC) film (open square), poly(EDOT-HQ-co-EDOT-PC) film electrocopolymerized at a feed composition of 10% EDOT-HQ and 90% EDOT-PC (filled triangle) and PEDOT film (open triangle) deposited on Au substrates, respectively. The scale bar represents 100 μm.

**Figure 5** shows a comparison of electrotoned cell behavior on poly(EDOT-HQ-co-EDOT-PC) and the PEDOT-OH control paired on patterned ITO glass. The ITO glass substrate was divided by an insulating gap to form isolated ITO glasses. The poly(EDOT-HQ-co-EDOT-PC) and poly(EDOT-OH) films were deposited onto one of the electrodes to fabricate a pair of heterogeneous electrodes (Figure S4a, Supporting Information).

The patterned ITO glasses were then assembled in our homemade electroculture device to culture the cells. Figure 5a shows the experimental approach to programmable control of cell attachment and detachment through the originally bioinert PEDOT material. The poly(EDOT-HQ-co-EDOT-PC) film was clearly very cell-resistant; in contrast, the NIH3T3 cells attached very well to the poly(EDOT-OH) film as a result of strong

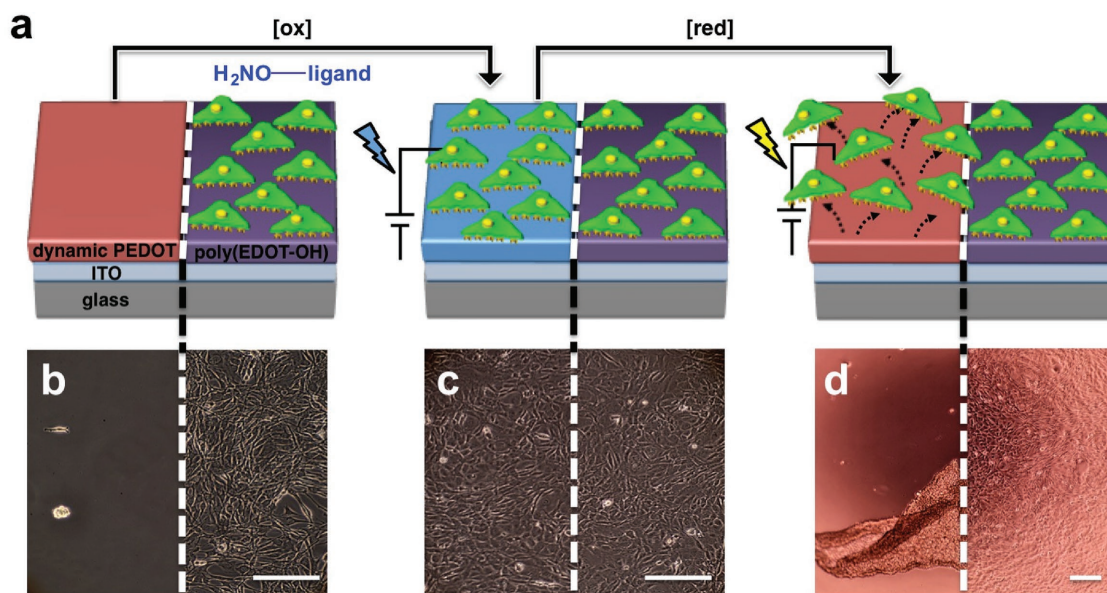


**Figure 5.** a) Schematic illustration of the controlled attachment and release of NIH3T3 cells on RGD peptide-conjugated poly(EDOT-HQ-co-EDOT-PC) film (electrocopolymerized at a feed composition of 10% EDOT-HQ and 90% EDOT-PC), compared with those nonspecifically attached to poly(EDOT-OH) controls paired on patterned ITO glass; b) poly(EDOT-HQ-co-EDOT-PC) films resist NIH3T3 cells in serum-supplemented medium, while PEDOT-OH controls bind cells well; c) after conjugated RGD was oxidized at +0.7 V versus Ag/AgCl, poly(EDOT-HQ-co-EDOT-PC) films strongly bound NIH3T3 cells at a cell density similar to that of PEDOT-OH controls; d) after cleavage of RGD peptide linkages upon reduction at -0.05 V versus Ag/AgCl, NIH3T3 cells are released from poly(EDOT-HQ-co-EDOT-PC) films. The scale bar represents 100 μm.



nonspecific binding (Figure 5b). The glass gap between the two polymer films also featured attached cells. After we applied an oxidation potential of 0.7 V, RGD peptides could be grafted onto a poly(EDOT-HQ-co-EDOT-PC) film via oxime ligation; thus, a high density of NIH3T3 cells strongly attached to and spread on the originally bioinert copolymer film (Figure 5c). This experiment definitively demonstrated specific cell attachment by an electrooxidation-induced ligand conjugation. After the cells were cultured for 24 h, we applied a reduction potential of  $-0.05$  V on both polymer films in 37 °C PBS buffer (pH 7.2). During this electroreduction process, the oxime linkages between RGD peptides and the poly(EDOT-HQ-co-EDOT-PC) films were cleaved, and the sites binding the attached cells to the poly(EDOT-HQ-co-EDOT-PC) films were subsequently lost. Within 15 min, a sheet of NIH3T3 cells detached from the poly(EDOT-HQ-co-EDOT-PC) electrode, while the NIH3T3 cells attached to the poly(EDOT-OH) electrode remained without any changes in their morphologies (Figure 5d). We then used a LIVE/DEAD viability/cytotoxicity kit and a Trypan blue exclusion assay to test the viability of the NIH3T3 cells; the viability of the detached cells was as high as 94%. This assay unambiguously demonstrated cell release by the electroreductive cleavage of ligands. Overall, the dynamic PEDOT film demonstrated its programmable control of cell attachment and release via electroresponsive specific binding. This dynamic PEDOT could be a potential source of electrode material to address the cell detachment issue of bioelectronic devices.

### 2.5. Efficient Electrical Communication and Stable Switching under Physiological Conditions

Nonfunctionalized PEDOT films serve as high-performance electrode materials in bioelectronic devices to communicate with (either stimulate or record) cells. As noted above, our dynamic PEDOT materials programmably control cell attachment and detachment, indicating their potential as ideal electronic materials in bioelectronic devices that integrate controlled cell–device communication and interaction (Figure 6a). However, their biocompatibility and electrical communication with nerve cells must be addressed in comparison with these properties in the nonfunctionalized PEDOT. Many previous studies have used the electrical stimulation of PC12 neurite outgrowth to evaluate the electrical performance of the organic electrode materials.<sup>[61]</sup> For a convenient comparison, we also adopted it as a simple assay to evaluate our dynamic PEDOT film. Similar to the aforementioned approach, we fabricated pairs of the dynamic PEDOT films furnished with RGD peptides in our homemade electroculture device and seeded PC12 cells onto the dynamic PEDOT materials under standard differentiation conditions. We then applied a biphasic pulse with an optimized amplitude ( $0.66$  mA cm<sup>-2</sup>) through the copolymers for 4 h per day for five consecutive days (Figure S4b, Supporting Information). We monitored the cell density and neurite length on the dynamic PEDOT films, with or without electrical stimulation, during the whole process. In addition, a nonfunctionalized PEDOT film was included as a control. After 5 d of culturing, the cell density values for all samples increase by more than one fold (Figure 6b).<sup>[62]</sup> When electrical stimulation was absent,

the cell density for the dynamic PEDOT film was 17.5% higher than that of the nonfunctionalized PEDOT control (Figure 6b). Moreover, when no electric signal was supplied to the dynamic PEDOT, the median neurite length of cells on the dynamic PEDOT was 23.4  $\mu$ m, which is 34.5% longer than that of the cells on the nonfunctionalized PEDOT control (17.4  $\mu$ m) (Figure 6c,d). Both results indicated the better biocompatibility of our dynamic PEDOT. With an electric signal was applied to the dynamic PEDOT for 5 d, the median neurite length of cells increased to 29.5  $\mu$ m (Figure 6c,e), corresponding to a 69.5% enhancement of neurite outgrowth when compared to that of the nonfunctionalized PEDOT. A statistical description of the results is provided in Figure S5 in the Supporting Information. After 5 d of applying the same electrical stimulation to the control, most of cells detached from the nonfunctionalized PEDOT film. These results definitely indicate that the dynamic PEDOT material could supply the combination of efficient communication and biocompatibility that is desired for bioelectronic devices.

Other concerns regarding our dynamic PEDOT include the switching stability after exposure to long-term electrical signals and the potential damage caused to differentiated cells during detachment from our dynamic PEDOT film. To estimate the stability of the oxime linkage during electrical communication with cells, we compared the cell density of PC12 cells under stimulation with their cell density without stimulation (Figure 6b). The cell density of the sample under stimulation remained higher than that without stimulation throughout the 5 d electrical stimulation period, and no loss of peptide ligands from stimulation was observed. The higher cell density of the stimulated sample might be due to the enhancement of cell proliferation by electrical stimulation. Furthermore, we did not observe a difference in cell loss during culturing of the two samples, with or without stimulation. However, we noted a distinctive cell loss when nonfunctionalized PEDOT was used as a substrate to culture cells during stimulation. These results indicate that the dynamic PEDOT material provides a reliable support for PC12 cells during electrical stimulation, which should be attributed to the stability of the oxime conjugation. To further verify this material's stability and dynamic functionality after stimulation, we applied a reductive potential of  $-0.05$  V for 15 min. The differentiated PC12 cells were completely released (Figure 6f) in response to electrocleaving the linkage to RGD peptides. These results further demonstrate that the integrity and function of the oxime linkage could survive electrical stimulation and culturing for 5 d. Stable switching under physiological conditions is critical for the long-term application of devices.

We used a LIVE/DEAD viability/cytotoxicity kit to examine the cell viability of PC12 cells and found that viability was as high as 93% (Figure S6, Supporting Information). After the cells released, we distributed the released PC12 cells in fresh culture medium and reseeded them into a culture dish. As shown in Figure 6g, PC12 cells spread well in the culture dish and fully extended their long neurites after 1 d of culturing. The high cell viability and well-maintained morphological integrity of the differentiated PC12 cells confirm that the electrocleavage of ligands can serve as a gentle detachment approach for differentiated cells. We expected these results, as the dynamic PEDOT material responds to a much lower potential ( $-0.05$  V)

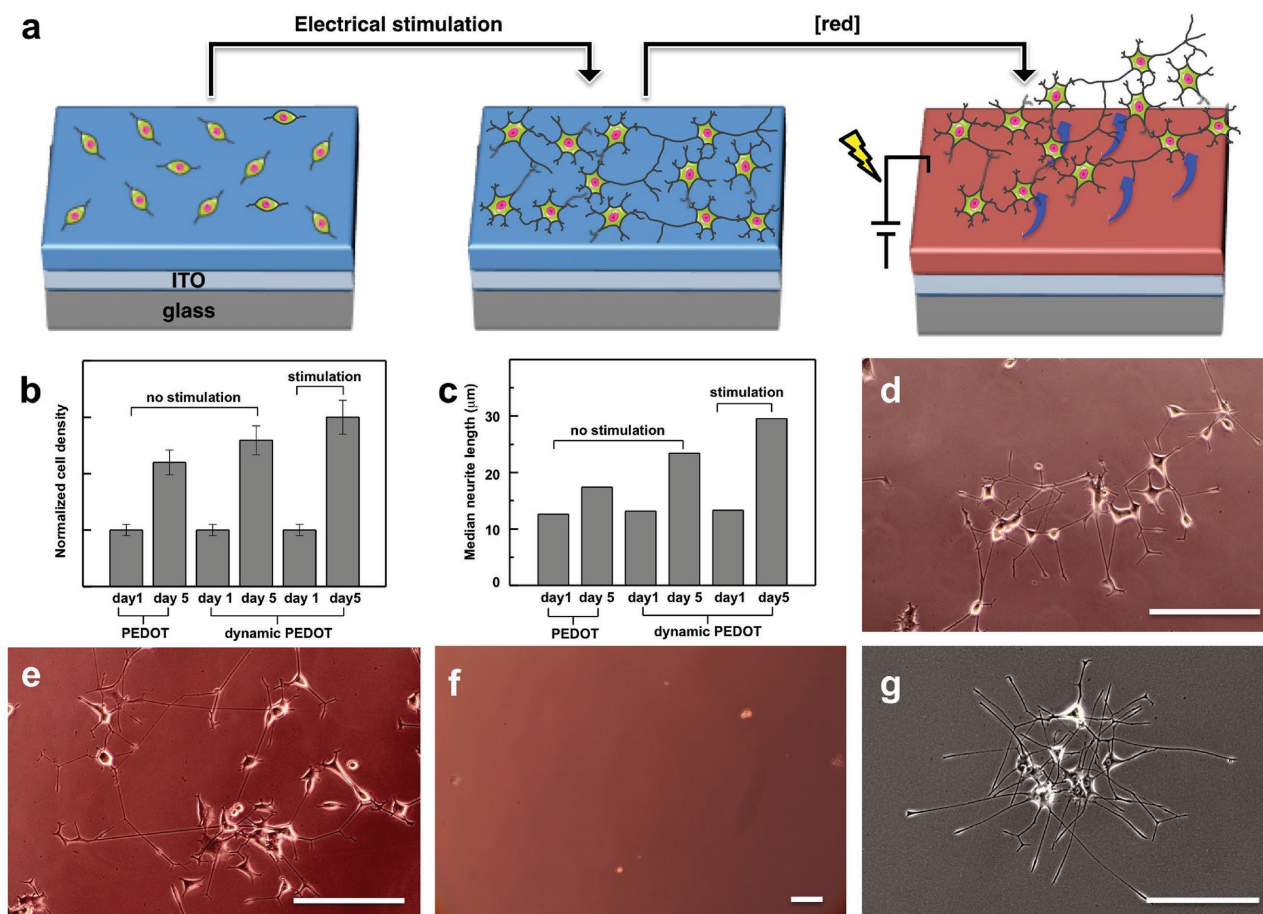


**Figure 6.** a) Schematic illustration of the experiment to demonstrate that dynamic linkages could survive during electrical communication between electrodes and neural cells. A 5 d long stimulation was applied to PC12 cells through the PEDOT electrode via programmed electrical pulses as a simple representation of the electrical communication between electrodes and neuronal cells; a reduction potential was subsequently applied to release cells. b) Normalized cell densities of PC12 cells differentiated on PEDOT and RGD-conjugated poly(EDOT-HQ-co-EDOT-PC) films, with and without electrical stimulation, for 1 and 5 d; c) median neurite length of PC12 cells differentiated on PEDOT and RGD-conjugated poly(EDOT-HQ-co-EDOT-PC) films, with and without electrical stimulation, for 1 and 5 d; bright-field images of PC12 cells on RGD-conjugated poly(EDOT-HQ-co-EDOT-PC) films d) without and e) with electrical stimulation by 60 mV biphasic pulses for 5 d in nerve growth factor (NGF)-supplemented medium; f) bright-field image for RGD-conjugated poly(EDOT-HQ-co-EDOT-PC) film after PC12 cell release by a reductive potential; g) bright-field image of released PC12 cells reseeded onto a culture dish in serum-containing media for 1 d. The scale bar represents 100 μm.

than the previous approach at 0.7 V, which demonstrated no damage to the cell membrane.<sup>[37]</sup> These results demonstrate that the electroresponsive oxime linkage is very stable during electrical stimulation, thus ensuring gentle, electrically tuned cell detachment with minimal damage to cell viability.

### 3. Conclusion

To meet the electrical communication, biocompatibility and attachment control requirements for advanced electronic devices, we have developed a dynamic conducting polymer that exhibits low impedance, resistance to nonspecific binding and stable redox-responsive specific cell-coupling. We have synthesized a hydroquinone-functionalized EDOT-based material and further copolymerized it with zwitterionic phosphorylcholine-functionalized EDOT to form a dynamic conducting polymer. Due to the benzoquinone–hydroquinone electroredox

interconversion, the dynamic PEDOT film possesses a clean electroresponsive oxime switch that may be used to address surface functions spatiotemporally. In addition, the dynamic PEDOT material, which has an optimized composition, is highly resistant to the nonspecific binding of proteins and cells, ensuring that the dynamic features and efficient communication can fully function in physiological environments. Moreover, the dynamic PEDOT material exhibits low impedance that is comparable to that of nonfunctionalized PEDOT and is particularly critical for high-resolution microarray devices. These features enable two favorable characteristics in the dynamic PEDOT. Electrooxidation of dynamic PEDOT initiates a strong specific interaction with targeted cells. When combined with nonspecific-binding resistance and low-impedance communication, the formation of a stable and efficient electrical interface with targeted cells is ensured. On the other hand, electroreduction restores the intrinsic bioinert material, which allows cells to be gently detached. Taking advantage of these two favorable

characteristics, we achieved efficient electrical stimulation of differentiation of model neuronal cells (PC12 cells) through the dynamic PEDOT for 4 h a day for five consecutive days, with greatly enhanced neurite growth and without cell loss. This material also cleanly released differentiated cells that maintained viability as high as 93% and morphological integrity. The dynamic and biomimetic PEDOT has potential use as a cell/tissue–electronic interface, which requires the efficient electrical communication, specific biofunction, and cell detachment control offered by this material. We are currently working on applications of this dynamic PEDOT to neural probes, conducting nerve regeneration conduits and PEDOT microarrays for multiplex cell sorting.

## 4. Experimental Section

**Materials:** EDOT and EDOT-OH were purchased from Sigma-Aldrich; the other chemicals and organic solvents for organic synthesis were purchased from Sigma-Aldrich and Wako Pure Chemical Industries. Aminoxy-functionalized RGD peptide (NH<sub>2</sub>O-EG<sub>2</sub>-GRGDSP) was produced by custom synthesis (Thinkpeptides); the culture medium, serum, growth factors, and aminoxy-functionalized Alexa-488 dyes were purchased from Invitrogen. All chemicals were of reagent grade and were used as received except dichloromethane and tetrahydrofuran (THF), which were dehydrated and purified using a PureSolv MD 5 Solvent Purification System (Innovative Technology). EDOT-PC was synthesized according to a reported procedure.<sup>[37]</sup>

**Synthesis of EDOT-HQ: Compound 1.** Hydroquinone (10.0 g, 90.8 mmol) was suspended in dichloromethane (100 mL). 3,4-Dihydro-2H-pyran (24.4 mL, 270 mmol) and pyridinium *p*-toluenesulfonate (4.52 g, 18 mmol) were added, and the mixture was stirred at room temperature overnight. The reaction mixture was quenched by addition of anhydrous K<sub>2</sub>CO<sub>3</sub> (1.0 g) and pyridine (1 mL). The reaction mixture was then washed with water (200 mL), dried with Na<sub>2</sub>SO<sub>4</sub>, and concentrated. The crude product was purified by recrystallization from ethyl acetate to afford white crystals (19.0 g, 76%). <sup>1</sup>H NMR (500 MHz, CDCl<sub>3</sub>): δ 6.97 (d, *J* = 1.0, 4H), 5.30 (t, *J* = 6.5, 2H), 3.93 (m, 2H), 3.58 (m, 2H), 1.99 (m, 2H), 1.84 (m, 2H), 1.63 (m, 8H). <sup>13</sup>C NMR (500 MHz, CDCl<sub>3</sub>): δ 151.9, 117.5, 117.5, 97.2, 62.1, 30.5, 25.3, 18.9 HRMS (EI) *m/z*: [M<sup>+</sup>] calcd for C<sub>16</sub>H<sub>22</sub>O<sub>4</sub>, 278.1518; found, 278.1516.

The white crystals (3.0 g 10.8 mmol) were then dissolved in 30 mL of dry THF. *Tert*-butyllithium (10 mL of a 1.6 M solution, 16.2 mmol) was added dropwise over 20 min at 0 °C. This mixture was stirred for 60 min and then slowly returned to room temperature over 1.5 h. 1,6-Dibromohexane (4.98 mL, 32.4 mmol) was added to the reaction. A white precipitate was immediately formed, and the mixture was continuously stirred for 12 h. The reaction mixture was then diluted with 100 mL of dichloromethane, washed with 50 mL of NH<sub>4</sub>Cl, and 50 mL of brine, dried over Na<sub>2</sub>SO<sub>4</sub>, and concentrated to yellow oil. Silica gel chromatography using gradient elution (15:1 hexane/ethyl acetate to 10:1 hexane/ethyl acetate) afforded the product (2.4 g, 51%) as a clear oil. <sup>1</sup>H NMR (500 MHz, CDCl<sub>3</sub>): δ 6.99 (m, 1H), 6.83 (m, 2H), 5.30 (t, *J* = 4.0 Hz, 2H), 3.92 (m, 2H), 3.58 (m, 2H), 3.40 (t, *J* = 7.0 Hz, 2H), 2.6 (t, *J* = 7.0 Hz, 2H), 1.95 (m, 2H), 1.85 (m, 2H), 1.63 (m, 8H), 1.44 (m, 2H), 1.38 (m, 2H). <sup>13</sup>C NMR (500 MHz, CDCl<sub>3</sub>): δ 151.4, 149.9, 132.9, 117.5, 115.3, 114.5, 97.1, 96.9, 62.1, 62.0, 34.0, 32.8, 30.7, 30.5, 30.4, 29.8, 28.6, 28.1, 25.3, 25.2, 19.0, 18.9 HRMS (EI) *m/z*: [M<sup>+</sup>] calcd for C<sub>22</sub>H<sub>33</sub>O<sub>3</sub>BrO<sub>4</sub>, 440.1562; found, 440.1562.

**Compound 2.** A mixture of NaH (0.74 g, 27.2 mmol) and 18-crown-6 ether (0.144 mg, 0.5 mmol) in 10 mL of anhydrous THF was stirred under nitrogen at 0 °C. 2,3-Dihydrothieno[3,4-*b*][1,4]dioxin-2-yl)methanol (Hydroxymethyl EDOT) (0.94 g, 5.5 mmol) in 15 mL of anhydrous THF was added. The mixture was stirred at room temperature for 1 h and then cooled down to 0 °C. **1** (2.4 g, 5.5 mmol) was added dropwise

for 10 min. After stirring at room temperature overnight, the mixture was diluted with 50 mL of NH<sub>4</sub>Cl aqueous solution. The mixture was extracted with dichloromethane (100 mL). The combined organic phases were washed with water, dried over Na<sub>2</sub>SO<sub>4</sub>, and evaporated in vacuo. The crude product was purified by flash chromatography (ethyl acetate/hexane = 1:6) to yield a colorless oil (2.12 g, 73%). <sup>1</sup>H NMR (500 MHz, CDCl<sub>3</sub>): δ 7.00 (dd, *J* = 8.5, 1.5 Hz, 1H), 6.85 (d, *J* = 3.0 Hz, 1H), 6.83 (dd, *J* = 8.5, 3.0 Hz, 1H), 6.32 (m, 2H), 5.30 (m, 2H), 4.29 (m, 1H), 4.24 (dd, *J* = 11.5, 2.0 Hz, 1H), 4.05 (dd, *J* = 12.0, 7.5 Hz, 1H), 3.93 (m, 2H), 3.67 (dd, *J* = 10.5, 5.0 Hz, 1H), 3.59 (m, 3H), 3.49 (t, *J* = 6.5 Hz, 2H), 2.60 (t, *J* = 7.5 Hz, 2H), 1.99 (m, 2H), 1.84 (m, 4H), 1.63 (m, 10H), 1.38 (m, 4H). <sup>13</sup>C NMR (500 MHz, CDCl<sub>3</sub>): δ 151.3, 149.7, 141.5, 141.4, 132.7, 118.3, 115.1, 114.3, 99.5, 99.4, 96.9, 96.7, 72.5, 71.9, 68.9, 66.1, 61.9, 61.8, 30.6, 30.4, 29.9, 29.3, 29.2, 25.8, 25.5, 25.2, 25.2, 18.9, 18.8 HRMS (EI) *m/z*: [M<sup>+</sup>] calcd for C<sub>29</sub>H<sub>40</sub>O<sub>7</sub>S, 532.2495; found, 532.2487.

**EDOT-HQ:** A solution of **2** (1.58 g, 3.0 mmol) in 125 mL of a 3:1:1 mixture of AcOH/THF/H<sub>2</sub>O was stirred for 4 h. The mixture was then concentrated, diluted in EtOAc (50 mL), washed with 1 × 10<sup>-3</sup> M NaOH (50 mL), and dried over Na<sub>2</sub>SO<sub>4</sub>. The crude product was purified by flash chromatography (ethyl acetate/hexane = 1:3) to yield a colorless oil (1.08 g, 99%). <sup>1</sup>H NMR (500 MHz, CDCl<sub>3</sub>): δ 6.63 (d, *J* = 8.0 Hz, 1H), 6.61 (d, *J* = 2.5 Hz, 1H), 6.54 (dd, *J* = 8.0, 2.5 Hz, 1H), 6.33 (m, 2H), 4.54 (s, 1H), 4.45 (s, 1H), 4.30 (m, 1H), 4.24 (dd, *J* = 11.5, 2.5 Hz, 1H), 4.06 (dd, *J* = 11.5, 7.5 Hz, 1H), 3.68 (dd, *J* = 10.5, 5.0 Hz, 1H), 3.60 (dd, *J* = 10.5, 6.0 Hz, 1H), 3.49 (t, *J* = 6.5 Hz, 2H), 2.54 (t, *J* = 7.5 Hz, 2H), 1.59 (m, 4H), 1.35 (m, 4H). <sup>13</sup>C NMR (500 MHz, CDCl<sub>3</sub>): δ 149.3, 147.3, 141.5, 141.5, 129.8, 116.8, 116.0, 113.3, 99.8, 99.6, 72.7, 71.9, 69.0, 66.2, 29.8, 29.4, 29.3, 29.0, 25.8 HRMS (EI) *m/z*: [M<sup>+</sup>] calcd for C<sub>19</sub>H<sub>24</sub>O<sub>5</sub>S, 364.1344; found, 364.1338.

**Electropolymerization and Electrochemical Analysis:** Electrochemical experiments were performed using an Autolab PGSTAT128N potentiostat (Metrohm Autolab) in a three-electrode electrochemical cell, with platinum as the counter electrode and Ag/AgNO<sub>3</sub> (0.01 M of AgNO<sub>3</sub> and 0.1 M of Bu<sub>4</sub>NPF<sub>6</sub> in acetonitrile) or Ag/AgCl (saturated KCl solution) as the reference electrode. Each measurement was calibrated using the standard ferrocene/ferrocenium redox system. Films of HQ-functionalized PEDOT, poly(EDOT-HQ), and PEDOT were electropolymerized in Au-dish electrodes using a degassed acetonitrile solution with 0.1 M LiClO<sub>4</sub> and 0.01 M monomer under ambient conditions through potential scans applied from -0.3 to +1.1 V versus Ag/AgNO<sub>3</sub>. Cyclic voltammograms of poly(EDOT-HQ) and PEDOT films were recorded in 1 M HClO<sub>4</sub> (pH 0) solution with applied cyclic potential scans from -0.3 to +0.7 V versus Ag/AgCl. To prepare poly(EDOT-HQ-co-EDOT-PC) films on ITO glass, a poly(EDOT-OH) film was first deposited onto ITO glass; the poly(EDOT-OH) film was immersed in an acetonitrile solution containing EDOT-HQ, phosphorylcholinemethyl-functionalized EDOT (EDOT-PC), and 0.1 M dioctyl sodium sulfosuccinate (surfactant), and the potential was scanned from -0.5 to +1.1 V versus Ag/AgNO<sub>3</sub>. Electrochemical impedance spectroscopy (EIS) was performed using a sinusoidal excitation signal with an excitation amplitude of 10 mV at 50 frequencies logarithmically spaced from 10 kHz to 1 Hz. The conducting polymer films used for measurements were coated on fresh Au substrates (area: 1 cm<sup>2</sup>). Before an EIS spectrum was recorded, samples were conditioned in PBS buffer at 0.23 V for 10 s. EIS was performed at 25 °C in the 1× PBS buffer with 10 × 10<sup>-3</sup> M [Fe(CN)<sub>6</sub>]<sup>3-/4-</sup> (1:1, mol/mol) as the redox couple.

**UV-vis Spectroelectrochemical Analysis:** In situ spectroelectrochemical measurements were recorded using a JASCO UV-630 spectrophotometer. Electropolymerization and spectroelectrochemical measurements of poly(EDOT-OH) and poly(EDOT-HQ) films were performed in an optical quartz cell equipped with a Pt counter electrode and Ag/AgNO<sub>3</sub> (0.01 M of AgNO<sub>3</sub> and 0.1 M of Bu<sub>4</sub>NPF<sub>6</sub> in acetonitrile) or Ag/AgCl (saturated KCl solution) as the reference electrode. ITO-coated quartz was first fixed within an optical quartz cell, which was then filled with an acetonitrile solution containing 0.01 M EDOT-OH monomer and 0.1 M LiClO<sub>4</sub>; cyclic voltammetry was performed in the potential range from -0.3 to +1.1 V versus Ag/AgNO<sub>3</sub> to deposit the poly(EDOT-OH) film onto the ITO-coated electrode. The monomer

solution was then removed, and the quartz cell was washed with acetonitrile. The spectroelectrochemical behavior of the poly(EDOT-OH) film was measured in 1 M HClO<sub>4</sub> (pH 0) solution versus Ag/AgCl electrode in the potential range from -0.3 to +0.7 V; the absorbance spectra were recorded as baselines. Next, 0.01 M EDOT-HQ monomer and 0.1 M LiClO<sub>4</sub> were dissolved in acetonitrile, and the solution was poured into the optical quartz cell; cyclic voltammetry was performed in the potential range from -0.3 to +1.1 V versus Ag/AgNO<sub>3</sub>, thereby depositing poly(EDOT-QH) films onto the poly(EDOT-OH) film. The spectroelectrochemical behavior of the double-layer polymer film was measured in 1 M HClO<sub>4</sub> (pH 0) solution versus Ag/AgCl electrode in the potential range from -0.3 to +0.7 V; after the baseline, which was the absorbance spectrum of the PEDOT-OH film, was subtracted, the absorbance spectrum of the poly(EDOT-HQ) film was obtained. The absorbance spectra recorded after the formation and cleavage of the oxime linkage on the poly(EDOT-HQ) film were obtained in the same way, as were the baselines for measurement.

**Immobilization of Fluorophores on Polymer-Deposited Macroelectrodes and Fluorophore Release:** The poly(EDOT-HQ) film was electrodeposited onto interdigitated electrodes (IDEs) with two sets of working electrodes (from BAS, Japan). The poly(EDOT-HQ)-coated IDEs were immersed in acetate buffer (pH 4.6), and a three-electrode electrochemical system was then used to selectively apply a constant voltage (0.7 V vs Ag/AgCl) to one or both of the working electrodes for 20 s. For conjugation of the aminoxy-functionalized Alexa-488 dyes to the polymer films, the oxidized polymer films were placed in acetate buffer (pH 4.6) containing 0.0002 M Alexa-488 dyes and 0.1 M aniline for 3 h. For release of the Alexa-488 dyes from the polymer films, the poly(EDOT-HQ)-coated IDE with the Alexa dyes on both working electrodes was placed in PBS buffer (pH 7.2), and a three-electrode electrochemical system was then used to apply a constant voltage of -0.05 V versus Ag/AgCl to a single working electrode for 15 min.

**Immobilization of Aminoxy-Functionalized RGD Peptide on a poly(EDOT-HQ-co-EDOT-PC) Film on ITO Glass:** The poly(EDOT-HQ-co-EDOT-PC)-coated ITO glass was immersed in acetate buffer (pH 4.6), and a three-electrode electrochemical system was then used to apply a constant voltage of 0.7 V versus Ag/AgCl to the copolymer film for 20 s. Next, the oxidized copolymer film was immersed for 12 h in acetate buffer (pH 4.6) containing 0.2 M RGD peptide (NH<sub>2</sub>O-EG<sub>2</sub>-GRGDSP) and 0.1 M aniline.

**Two-Photon Imaging:** Two-photon imaging of the Alexa-488 dyes on the poly(EDOT-HQ)-coated interdigitated electrodes was performed using an Olympus BX-61 microscope equipped with a water immersion lens (60 $\times$ ; NA = 0.9; Olympus, Japan), an FV1000 scanner (Olympus, Japan), and an ultrafast, pulsed (<140 fs), tunable (720–930 nm) laser (Chameleon; Coherent, USA). The Alexa Fluor 488 emission was excited at 830 nm and collected by a photomultiplier (PMT) with a 570 nm dichroic mirror followed by a bandpass filter (495–540 nm).

**Cell Culture and Differentiation:** Rat pheochromocytoma (PC12) and NIH3T3 cells were obtained from the RIKEN Cell Bank. PC12 cells were seeded directly onto polymer substrates (densities: 5–100  $\times 10^3$  mm<sup>-2</sup>) and cultured normally in Dulbecco's modified Eagle medium (DMEM) supplemented with 10% horse serum and 10% fetal bovine serum (FBS) at 37 °C in a humidified atmosphere containing 5% CO<sub>2</sub>. To induce neural differentiation, DMEM medium containing 50 ng mL<sup>-1</sup> NGF 2.5S was used. The DMEM medium for the normal culture was replaced every 3 d, and that for differentiation was refreshed every 2 d. NIH3T3 cells were seeded directly onto polymer substrates (densities: 100–250  $\times 10^3$  mm<sup>-2</sup>) and cultured normally in DMEM supplemented with 10% FBS at 37 °C in a humidified atmosphere containing 5% CO<sub>2</sub>. The culture medium for the NIH3T3 cells was replaced every 2 d.

Because EDOT polymer thin films are transparent, optical microscopy and quantitative image analysis tools could be used to quantify cell-material interactions. Images from the microscope were acquired using a CMOS camera (D90; Nikon) and were analyzed using ImageJ software.

**Electrical Stimulation and Release:** After the above procedures for cell differentiation were followed, PC12 cells were seeded at a density of 2  $\times 10^4$  mm<sup>-2</sup> on EDOT polymer thin films deposited onto ITO glass

substrates assembled in a homemade culture chamber (Figure S2a, Supporting Information) and then incubated for 12 h to ensure their attachment and spreading prior to the initiation of electrical stimulation. The ITO substrate was separated into two equal parts by a 400  $\mu$ m insulating linear gap (fabricated through confined acid etching). A charge-balanced biphasic electrical stimulation at 250 Hz (Figure S2b, Supporting Information) was produced using a B2912A precision source/measure unit (Agilent); the two parts of the EDOT-polymer-coated ITO substrate served as electrodes to release electrical signals to the cells. The major advantage of the biphasic electrical stimulation was that it could maintain a charge balance while minimizing most cell damage. After the initial 12 h of incubation, the PC12 cells were subjected to electrical stimulation for more than 5 d (4 h per day). The amplitude of each biphasic pulse was 60 mV. PC12 cells plated on the same PEDOT thin films, but not subjected to any electrical stimulation, served as controls. The morphological features of all cells were examined every 24 h.

To release the PC12 and NIH3T3 cells from the dynamic PEDOT films, the original culture medium was carefully removed, and PBS buffer was then added gently to the homemade culture devices. A low potential (-0.05 V vs Ag/AgCl) was applied to the dynamic copolymer film for 15 min. The PBS buffer in the homemade devices was replaced with the culture medium, and the cells were then detached in an incubator at 37 °C.

**Neurite Parameters—Definition, Measurements, and Analysis:** Captured cell images were processed and analyzed using ImageJ software. Neurite length was defined as the actual length from the tip of the neurite to the junction between the cell body and neurite base; it was traced manually with a cursor and calibrated to standards. In the case of a branched neurite, the length of the longest branch was measured from the tip of the neurite to the cell body; the length of short branches was measured from the tip of the neurite to the neurite branch point. The actual distributions of neurite lengths, along with the population median, are reported for each condition.

**Cell Viability:** A LIVE/DEAD viability/cytotoxicity kit (Invitrogen) and a Trypan blue exclusion assay (Sigma) were used to detect the viability of NIH3T3 and PC12 cells released from the polymer surfaces.

**LIVE/DEAD Viability/Cytotoxicity Kit:** Following the example protocol, a labeling solution (10 mL) was made containing  $\approx 2 \times 10^{-6}$  M calcein AM and  $4 \times 10^{-6}$  M EthD-1. A 2 mL portion of the labeling solution was added to the PBS buffer with the released cells, and the mixture was incubated at room temperature for 20–40 min. Following incubation, a 10  $\mu$ L portion of fresh labeling solution was separated and placed on a clean microscope slide. Using fine-tipped forceps, the slide was carefully (but quickly) inverted, and a wet cover slip was mounted onto the microscope slide. Finally, the live and dead labeled cells were counted using a fluorescence microscope. The number of viable cells was calculated as a percentage by dividing the number of living cells by the total number of cells.

**Trypan Blue Exclusion Assay:** The released NIH3T3 and PC12 cells were incubated with a diluted (0.4%, w/v) Trypan blue solution (Sigma) for 2–3 min at room temperature. Cell viability was determined using a hemocytometer. The cell survival percentage for each treatment group was determined by counting the dead and live cells. The number of viable cells was calculated as a percentage by dividing the number of living cells by the total number of cells.

## Supporting Information

Supporting Information is available from the Wiley Online Library or from the author.

## Acknowledgements

This study was supported by the RIKEN Advanced Science Institute, a Grant-in-Aid for Young Scientists (No. 22681016) from JSPS/MEXT,

Japan, NSFC (21474014), Fundamental Research Funds for the Central Universities (2232015A3-01), the NSF of Shanghai (14ZR1400200, China), MOST 104-2113-M-002-019-MY2 (Taiwan), and Academia Sinica under grant AS-104-TP-A11. Dr. B.Z. thanks RIKEN for a Special Postdoctoral Researcher Fellowship.

## Conflict of Interest

The authors declare no conflict of interest.

## Keywords

low impedance electronics, organic bioelectronics, PEDOT, redox-switchable materials, smart materials

Received: July 13, 2017

Revised: October 7, 2017

Published online: January 15, 2018

- [1] R. van den Brand, J. Heutschi, Q. Barraud, J. DiGiovanna, K. Bartholdi, M. Huerlimann, L. Friedli, I. Vollenweider, E. M. Moraud, S. Duis, N. Dominici, S. Micera, P. Musienko, G. Courtine, *Science* **2012**, 336, 1182.
- [2] J. E. O'Doherty, M. A. Lebedev, P. J. Ifft, K. Z. Zhuang, S. Shokur, H. Bleuler, M. A. L. Nicoletis, *Nature* **2011**, 479, 228.
- [3] T. Aflalo, S. Kellis, C. Klaes, B. Lee, Y. Shi, K. Pejsa, K. Shanfield, S. Hayes-Jackson, M. Aisen, C. Heck, C. Liu, R. A. Andersen, *Science* **2015**, 348, 906.
- [4] L. R. Hochberg, D. Bacher, B. Jarosiewicz, N. Y. Masse, J. D. Simeral, J. Vogel, S. Haddadin, J. Liu, S. S. Cash, P. van der Smagt, J. P. Donoghue, *Nature* **2012**, 485, 372.
- [5] W. Gao, S. Emaminejad, H. Y. Y. Nyein, S. Challa, K. Chen, A. Peck, H. M. Fahad, H. Ota, H. Shiraki, D. Kiriya, D.-H. Lien, G. A. Brooks, R. W. Davis, A. Javey, *Nature* **2016**, 529, 509.
- [6] H. Lee, C. Song, Y. S. Hong, M. S. Kim, H. R. Cho, T. Kang, K. Shin, S. H. Choi, T. Hyeon, D.-H. Kim, *Sci. Adv.* **2017**, 3, e1601314.
- [7] R. O. Becker, *Nature* **1972**, 235, 109.
- [8] S. Hamid, R. Hayek, *Eur. Spine J.* **2018**, 17, 1256.
- [9] M. Zhao, B. Song, J. Pu, T. Wada, B. Reid, G. Tai, F. Wang, A. Guo, P. Walczysko, Y. Gu, T. Sasaki, A. Suzuki, J. V. Forrester, H. R. Bourne, P. N. Devreotes, C. D. McCaig, J. M. Penninger, *Nature* **2006**, 442, 457.
- [10] S. Cogan, *Annu. Rev. Biomed. Eng.* **2008**, 10, 275.
- [11] S. Wilks, S. Richardson-Burns, J. Hendricks, D. Martin, K. Otto, *Front. Neuroeng.* **2009**, 2, 7.
- [12] R. Biran, D. Martin, P. Tresco, *Exp. Neurol.* **2005**, 195, 115.
- [13] W. Grill, S. Norman, R. Bellamkonda, *Annu. Rev. Biomed. Eng.* **2009**, 11, 1.
- [14] C. Xie, J. Liu, T.-M. Fu, X. Dai, W. Zhou, C. M. Lieber, *Nat. Mater.* **2015**, 14, 1286.
- [15] I. R. Mineev, P. Musienko, A. Hirsch, Q. Barraud, N. Wenger, E. M. Moraud, J. Gandar, M. Capogrosso, T. Milekovic, L. Asboth, R. F. Torres, N. Vachicouras, Q. Liu, N. Pavlova, S. Duis, A. Larmagnac, J. Voeroes, S. Micera, Z. Suo, G. Courtine, S. P. Lacour, *Science* **2015**, 347, 159.
- [16] T. D. Y. Kozai, N. B. Langhals, P. R. Patel, X. Deng, H. Zhang, K. L. Smith, J. Lahann, N. A. Kotov, D. R. Kipke, *Nat. Mater.* **2012**, 11, 1065.
- [17] R. Green, N. Lovell, L. Poole-Warren, *Biomaterials* **2009**, 30, 3637.
- [18] R. T. Hassarati, J. A. Goding, S. Baek, A. J. Patton, L. A. Poole-Warren, E. A. Green, *J. Polym. Sci., Part B: Polym. Phys.* **2014**, 52, 666.
- [19] M. R. Abidian, D. C. Martin, *Biomaterials* **2008**, 29, 1273.
- [20] N. K. Guimard, N. Gomez, C. E. Schmidt, *Prog. Polym. Sci.* **2007**, 32, 876.
- [21] K. Ludwig, J. Uram, J. Yang, D. Martin, D. Kipke, *J. Neural Eng.* **2006**, 3, 59.
- [22] X. Cui, D. Zhou, *IEEE Trans. Neural Syst. Rehabil. Eng.* **2007**, 15, 502.
- [23] Y. Hitoshi, O. Masaki, W. Wolfgang, *J. Electroanal. Chem.* **1995**, 397, 163.
- [24] S. Venkatraman, J. Hendricks, S. Richardson-Burns, E. Jan, D. Martin, J. M. Carmena, in *the 4th Int. IEEE EMBS Conf. on Neural Engineering*, **2009**, pp. 383.
- [25] S.-C. Luo, J. Sekine, B. Zhu, H. Zhao, A. Nakao, H.-H. Yu, *ACS Nano* **2012**, 6, 3018.
- [26] R. Green, P. Matteucci, R. Hassarati, B. Giraud, C. Dodds, S. Chen, P. Byrnes-Preston, G. Suaning, L. Poole-Warren, N. Lovell, *J. Neural Eng.* **2013**, 10, 016009.
- [27] M. Simon Edward, H. Michael John, K. Robert Michail Ivan, W. Gordon George, *Adv. Funct. Mater.* **2012**, 22, 2003.
- [28] S. Yang, B. Kim, A. Zakhidov, P. Taylor, J.-K. Lee, C. Ober, M. Lindau, G. Malliaras, *Adv. Mater.* **2011**, 23, H184.
- [29] P. Lin, F. Yan, J. Yu, H. Chan, M. Yang, *Adv. Mater.* **2010**, 22, 3655.
- [30] J. Isaksson, P. Kjäll, D. Nilsson, N. Robinson, M. Berggren, A. Richter-Dahlfors, *Nat. Mater.* **2007**, 6, 673.
- [31] D. Khodagholy, T. Doublet, P. Quilichini, M. Gurfinkel, P. Leleux, A. Ghestem, E. Ismailova, T. Hervé, S. Sanaur, C. Bernard, G. G. Malliaras, *Nat. Commun.* **2013**, 4, 1575.
- [32] J. Chikar, J. Hendricks, S. Richardson-Burns, Y. Raphael, B. Pflugst, D. Martin, *Biomaterials* **2012**, 33, 1982.
- [33] M. R. Abidian, K. A. Ludwig, T. C. Marzullo, D. C. Martin, D. R. Kipke, *Adv. Mater.* **2009**, 21, 3764.
- [34] S.-C. Luo, E. Mohamed Ali, N. C. Tansil, H.-h. Yu, S. Gao, E. A. B. Kantchev, J. Y. Ying, *Langmuir* **2008**, 24, 8071.
- [35] J. Rivnay, P. Leleux, M. Ferro, M. Sessolo, A. Williamson, D. A. Koutsouras, M. R. Dion Khodagholy, X. Strakosas, R. M. Owens, C. Benar, J.-M. Badier, C. Bernard, G. G. Malliaras, *Sci. Adv.* **2016**, e1400251.
- [36] C.-H. Chen, S.-C. Luo, *ACS Appl. Mater. Interfaces* **2015**, 7, 21931.
- [37] K. A. Ludwig, J. D. Uram, J. Yang, D. C. Martin, D. R. Kipke, *J. Neural Eng.* **2006**, 3, 59.
- [38] A. J. Hackett, J. Malmström, J. Travas-Sejdic, *Prog. Polym. Sci.* **2017**, 70, 18.
- [39] M. Bongo, O. Winther-jensen, S. Himmelberger, X. Strakosas, M. Ramuz, A. Hama, E. Stavrinidou, G. G. Malliaras, A. Salleo, B. Winther-Jensen, R. M. Owens, *J. Mater. Chem. B* **2013**, 1, 3860.
- [40] L. Ouyang, B. Wei, C.-c. Kuo, S. Pathak, B. Farrell, D. C. Martin, *Sci. Adv.* **2017**, 3, e1600448.
- [41] B. Zhu, S.-C. Luo, H. Zhao, H.-A. Lin, J. Sekine, A. Nakao, C. Chen, Y. Yamashita, H.-h. Yu, *Nat. Commun.* **2014**, 5, 4523.
- [42] J. Rivnay, H. Wang, L. Fenno, K. Deisseroth, G. G. Malliaras, *Sci. Adv.* **2017**, 3, e1601649.
- [43] K. Uto, J. H. Tsui, C. A. DeForest, D.-H. Kim, *Prog. Polym. Sci.* **2017**, 65, 53.
- [44] Y.-S. Hsiao, B.-C. Ho, H.-X. Yan, C.-W. Kuo, D.-Y. Chueh, H.-h. Yu, P. J. Chen, *Mater. Chem. B* **2015**, 3, 5103.
- [45] O. Guillaume-Gentil, M. Gabi, M. Zenobi-Wong, J. Vörös, *Biomed. Microdevices* **2011**, 13, 221.
- [46] Y. Arisaka, J. Kobayashi, M. Yamato, Y. Akiyama, T. Okano, *Biomaterials* **2013**, 34, 4214.
- [47] J. You, J. S. Heo, J. Kim, T. Park, B. Kim, H.-S. Kim, Y. Choi, H. O. Kim, E. Kim, *ACS Nano* **2013**, 7, 4119.
- [48] H. Y. Yoshikawa, F. F. Rossetti, S. Kaufmann, T. Kaindl, J. Madsen, U. Engel, A. L. Lewis, S. P. Armes, M. Tanaka, *J. Am. Chem. Soc.* **2011**, 133, 1367.

- [49] K. M. Persson, S. Lönnqvist, K. Tybrandt, R. Gabrielsson, D. Nilsson, G. Kratz, M. Berggren, *Adv. Funct. Mater.* **2015**, 25, 7056.
- [50] K. M. Persson, R. Karlsson, K. Svennersten, S. Löffler, E. W. H. Jager, A. Richter-Dahlfors, P. Konradsson, M. Berggren, *Adv. Mater.* **2011**, 23, 4403.
- [51] M. Y. Okamura, G. Feher, *Annu. Rev. Biochem.* **1992**, 61, 861.
- [52] M. Quan, D. Sanchez, M. F. Wasylkiw, D. K. Smith, *J. Am. Chem. Soc.* **2007**, 129, 12847.
- [53] G. Milczarek, O. Inganas, *Science* **2012**, 335, 1468.
- [54] W.-S. Yeo, M. Mrksich, *Langmuir* **2006**, 22, 10816.
- [55] S. Park, N. P. Westcott, W. Luo, D. Dutta, M. N. Yousaf, *Bioconjugate Chem.* **2014**, 25, 543.
- [56] C. Karlsson, H. Huang, M. Strømme, A. Gogoll, M. Sjödin, *J. Phys. Chem. C* **2014**, 41, 23499.
- [57] Sirajuddin, M. I. Bhanger, A. Niaz, A. Shah, A. Rauf, *Talanta* **2007**, 72, 546.
- [58] W. Luo, N. P. Westcott, A. Pulsipher, M. N. Yousaf, *Langmuir* **2008**, 24, 13096.
- [59] T. Moro, Y. Takatori, K. Ishihara, T. Konno, Y. Takigawa, T. Matsushita, U. I. Chung, K. Nakamura, H. Kawaguchi, *Nat. Mater.* **2004**, 3, 829.
- [60] J. Fang, B. H. Wallikewitz, F. Gao, G. Tu, C. Müller, G. Pace, R. H. Friend, W. T. S. Huck, *J. Am. Chem. Soc.* **2011**, 133, 683.
- [61] L. Ghasemi-Mobarakeh, M. P. Prabhakaran, M. Morshed, M. H. Nasr-Esfahani, H. Baharvand, S. Kiani, S. S. Al-Deyab, S. Ramakrishna, *J. Tissue Eng. Regener. Med.* **2011**, 5, e17.
- [62] L. A. Greene, A. S. Tischler, *Proc. Natl. Acad. Sci. USA* **1976**, 73, 2424.